Journal of Analytical and Applied Pyrolysis 169 (2023) 105861

Contents lists available at ScienceDirect

Journal of Analytical and Applied Pyrolysis

journal homepage: www.elsevier.com/locate/jaap

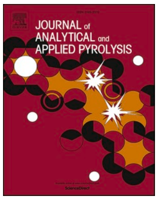

How height-related variations in hybrid poplars affect composition and pyrolytic behaviour: The key role of lignin maturity during woody-biomass pyrolysis

M.B. Folgueras [a], J.M. Gómez-Martín [a,b], M.A. Diez [b,*]

[a] *Energy Department, University of Oviedo, School of Mining, Energy and Materials Engineering, Independencia 13, 33004 Oviedo, Spain*
[b] *Institute of Science and Technology of Carbon (INCAR), CSIC, Francisco Pintado Fe 26, 33011 Oviedo, Spain*

ARTICLE INFO

Keywords:
Hybrid poplars
Short Rotation Woody Coppice
Thermogravimetry
FTIR indices
Biomass component interactions
Lignin maturity

ABSTRACT

This work aims to explore the height-related changes in chemical composition, calorific value, and thermochemical behavior during pyrolysis of four types of hybrid poplars (AF2, Beaupré, I214 and Monviso) and their structural components. The samples were collected from a Short Rotation Woody Coppice (SRWC) located in an abandoned opencast mine in the north of Spain. The effect of lignin and extractives (hydrophilic and hydrophobic ones) on wood pyrolysis, as well as the relationships between thermochemical properties and lignocellulosic composition, extractive content and lignin maturity, are investigated. The higher bark content of the top sections influences chemical and structural compositions. They have higher calorific values and more lignin, extractives, N and S contents, yielding more fixed carbon and ash. Additionally, the lignin of the top sections is less thermally stable. The isolation of structural components from the samples shifts the maximum volatile emission to higher temperatures for lignin and lower temperatures for holocellulose and cellulose, compared with those in the un-extracted samples. Lignin has a notable influence on wood decomposition since: (i) until its β-O-4 linkages and hemicellulose/lignin connections have been broken, cellulose devolatilization does not reach its maximum rate; and (ii) its removal reduces sample thermal stability, its effect being more significant than that of extractive removal. DRIFT spectroscopy is a valuable technique for predicting variations in chemical and thermochemical characteristics with the height of the wood sample. Several indices representing ratios of the maximum absorbance of specific signatures of lignin and cellulose could be appropriate for quick preliminary screening of woody biomass.

1. Introduction

Biomass production on contaminated land, especially in large-degraded areas, such as abandoned coal mines, can be a temporary solution for these sites and host potential for renewable energy transition to replace fossil fuels. The use of these zones avoids the competition between energy and food crops and, at the same time, it contributes to pollution control through phytostabilisation and economic reactivation [1] and captures greenhouse gases by plant growth and carbon retention in soil [2].

Genus *Populus* (poplars) is a group of trees highly used for Short Rotation Woody Coppices (SRWC) due to their rapid growth, resistance to environmental stress [3], adaptation to degraded soils with few nutrients, and acceptable biomass yields [4]. Therefore, this type of biomass can be suitable for obtaining some chemical products by pyrolysis. By applying low-temperature pyrolysis, biomass is transformed into valuable chemical products, biomaterials, and biofuels. This thermochemical process between 170 and 500 °C involves numerous intermediates and overlapping steps that depend on several factors such as the compositional distribution of structural and non-structural components, particle size, decomposition temperature, heating rate, and residence time [5].

Thermogravimetry is recognized as a proper analytical technique to explore the thermal behaviour of woody biomass during pyrolysis and combustion. Several researchers [6–10] have studied the behaviour of *Populus* during pyrolysis by thermogravimetry. Meszaros et al. [7] used young shoots of different hardwood species (poplar, black locust, and willow) and an herbaceous plant (Miscanthus sinensis), obtaining

---

* Corresponding author.
E-mail address: madiez@incar.csic.es (M.A. Diez).

https://doi.org/10.1016/j.jaap.2023.105861
Received 10 August 2022; Received in revised form 3 January 2023; Accepted 5 January 2023

similar thermal behaviour in both oxidative and inert atmospheres. They pointed out that further research is necessary to understand the impact of tree age and soil characteristics on woody biomass thermal behaviour. During the pyrolysis process of nine different poplar clones from short rotation coppice (SRC), a synergistic effect was reported from the simultaneous decomposition of cellulose and lignin [9].

Chemical properties and thermochemical behaviour of wood from poplars change depending on the genotype [2], the characteristics of the soil [4] and those of the environment, the age of the tree, as well as from one part to another of the tree [11]. Although these variations can be slight, they are essential for adapting the chemical or enzymatic processes needed for converting this type of biomass into valuable chemical products or biofuels. Hence, more efficient strategies can be applied, and products with better quality and properties can be obtained. In spite of its importance, there are few research studies on the variations of the chemical and thermochemical properties of different parts of poplars [11,12]. Álvarez-Álvarez et al. [11] analyzed different fractions of poplars (wood, bark and crown) and the whole tree, comparing their energy potential with those of other tree species. They concluded that the properties of biomass depend on the species and genetic material considered. Gómez-Martín et al. [12] reported differences in ash yield, heating value and pyrolytic behaviour from the base to the top of three hybrid poplars.

On the other hand, Chaves et al. [13] studied longitudinal and radial variations of extractive and lignin contents in *Eucalyptus*, and they found that both increase at positions closer to the base of the tree. Palacka et al. [14] focused their research on evaluating the properties as a fuel of different parts of *Picea abies* (roots, bark and wood of the trunk, branches, needles and cones) and concluded that they could vary significantly.

As the previous research shows, variations of wood chemical properties exist along the tree's height. Also, differences in chemical structure, linkages and functional group relative abundance affect the properties of the biomass polymers [15]. This topic has been scarcely studied [11–14], although this knowledge would allow us to optimize the thermal and/or biological treatment according to the objective looked for and to choose those parts of the tree more adequately. In a non-scale economy and for some cases, a suitable selection of the required part of a tree would allow us to avoid cutting down the whole tree, thereby reducing its damage. Additionally, as extractive and lignin contents vary substantially with height [13], it is necessary to improve knowledge about the effect of these components on lignocellulosic biomass pyrolysis. Although there are many studies about the extractive influence on biomass behavior during pyrolysis [10,16–18], less attention has been paid to the effect of lignin on cellulose thermal stability [9]. Rego et al. [9] observed a positive linear relationship between Kissinger energy activation of biomass and lignin content, suggesting a synergistic effect between holocellulose and lignin. Thus, higher lignin content decomposing at the same time as cellulose improves wood resistance to pyrolysis, probably because lignin reinforces the cohesion of hemicellulose and cellulose fibers [9]. They also recognized that more research effort on this topic is necessary [9].

As mentioned, there are two aspects of woody biomass pyrolysis that need a bigger research effort and, consequently, they are the main objectives of this research: (i) the study of the variations of biomass composition and pyrolytic behavior with height of tree; and (ii) the evaluation of the role and importance of lignin on biomass thermal stability during pyrolysis.

As previous research on *Eucalyptus* has shown [13], there are significant variations of lignin content with tree height, which can help to a better understanding of lignin role in biomass pyrolysis. Thus, the structure of this article is oriented to evaluate if, in hybrid poplars, lignin is a key element in compositional height-related variations and its significance in pyrolysis. Accordingly, after analyzing the chemical and structural composition and extractive content, the next step is the study of the lignin role on biomass thermal stability, which implies the evaluation of the pyrolytic behavior of the whole samples and their isolated components as well as the effect of lignin (compared to extractives) on biomass thermal stability. Finally, and associated with lignin significance, mathematical expressions based on lignin content and its chemical structure that allows us to predict the thermal properties of biomass are proposed.

The applications of these results may contribute to the following: (i) a better selection of the parts of the trees for obtaining valuable chemical products or for its thermal valorization; (ii) an improvement of pyrolysis models through a better knowledge of lignin role in this process; and (iii) a more accurate prediction of heating values and ash yields of woody biomass, which would allow us to implement better automation of thermal processes. All these practical implications may help to reduce costs and improve sustainability by using biomass as a feedstock or an energy source.

For this research, samples at three heights – top, middle and base- of four hybrid clones of the genotypes AF2, Beaupré, I214 and Monviso with a rotation cycle ranging from 5 to 9 years were collected and used.

2. Materials and methods

2.1. Materials

The lignocellulosic biomass used in this study came from a short-rotation plantation of a former opencast coal mine site in El Cantil-Asturias, northern Spain [19]. The tree species investigated were four hybrid poplars currently used in short rotation coppice plantations (SRC) as feedstock for bioenergy production: AF2 (*Populus nigra* x *Populus deltoides*), Beaupré (*Populus deltoides* x *Populus trichocarpa*), I214 (*Populus nigra* x *Populus deltoides*) and Monviso (*Populus generosa* x *Populus nigra*). AF2 and Monviso (Mo) were cut after a growth cycle of 5 years, while the growth cycles for Beaupré (Be) and I214 were 9 and 8 years, respectively. Wood samples from each hybrid were sorted into three different parts: base (B), middle (M), and top (T) branches (Fig. S1). The cut sections without any foliage or roots were dried by forced air circulation at 35 °C for 48 h to reduce the moisture content to 3.9–5.6 wt%. Gross samples of each hybrid poplar section were reduced in size and homogenized to obtain samples with two different particle sizes < 0.212 and < 1 mm. Samples with a size particle < 1 mm were used for determining lignocellulosic composition, while those < 0.212 mm were used for the rest of the analysis (proximate and ultimate analysis, HHV, FTIR, and thermogravimetry). The particle morphology of the ground samples was short and chipped.

2.2. Raw biomass characteristics

Proximate analysis was performed to classify the fuels according to their thermochemical composition, moisture, volatile matter, and ash contents, following the ISO 18134–1:2015, ISO 18123:2015 and ISO 18122:2015 standards, respectively. After drying and devolatilization (fixed carbon, FC), the ash-free carbon-rich solid was calculated by subtracting the percentages of moisture, ash and volatile matter from 100%. The ultimate analysis was carried out using a LECO CHN-2000 for C, H and N (ISO 29541), and a LECO S-144 DR was employed for total sulfur (ISO 19579). The oxygen content was calculated from the mass balance. The elementary microanalyses of the ashes obtained at 550 °C of raw and extractive-free samples were obtained using a scanning electron microscope equipped with an energy dispersive X-ray analyser (SEM-EDX). A set of microphotographs of different areas and spots were randomly chosen, recording the EDX analysis. An IKA C4000 adiabatic bomb calorimeter was used to determine the high heating value (HHV) and to calculate the low heating value (LHV) of all the samples, according to the ISO 1928:2009 standard procedure. In this research, HHV values were not only measured but also calculated by using the mathematical models developed by Channiwala and Parikh [20] and Degroot and Shafizadeh [21], which are based on elemental analysis and lignocellulosic compositions of biofuels, respectively. For most of the samples, experimental data agree with the calculated ones, the deviation being lower than 5%.

2.3. Lignocellulosic composition

Structural and non-structural components were extracted from the samples. Extractives were isolated from each sample by successive extractions with acetone in a Soxhlet apparatus ($E_{acetone}$) and hot water under reflux (E_{water}), according to the Technical Association of the Pulp and Paper Industry -TAPPI- (TAPPI T204 om-88, and TAPPI T207 om-93, respectively). Structural analysis of the extractive-free dry samples was carried out according to the guidelines in several chemical protocols. Briefly, holocellulose was isolated by the delignification process developed by Wise et al. [22]. The holocellulose content was determined through successive acid chlorination cycles with sodium chlorite and glacial acetic acid at 70–80 °C to remove the lignin, while carbohydrates remained. The change in color from light brown to white indicated the level of delignification. The holocellulose obtained was filtered, washed with distilled water, and dried. Subsequently, the resulting delignified holocellulose was treated using a 1% aqueous NaOH solution to isolate α-cellulose as an insoluble fraction (TAPPI T212 om-02). The hemicellulose content was obtained from the mass balance of holocellulose and cellulose quantities. Klason lignin (acid-insoluble lignin) was separated by two-stage acidic hydrolysis of extractive-free samples (TAPPI T222 om-02). In the first stage, a 72% w/w H_2SO_4 solution at 30 °C for 1 h was used to promote the structural rupture of lignocellulosic material and hydrolyze the polymeric polysaccharides into oligosaccharides. This stage is followed by dilution with water and secondary acid hydrolysis with a 4% w/w H_2SO_4 solution to break oligosaccharides into soluble monosaccharides, while the lignin remains as a solid fraction that is vacuum filtered and measured gravimetrically.

2.4. Thermogravimetric (TG) analysis

The samples were pyrolyzed using a Mettler Toledo TGA/DSC1 Star System TGA/DSC1 thermoanalyzer. Representative samples of about 5 mg with a particle size lower than 212 μm were evenly distributed in an open platinum crucible and then heated from room temperature to 800 °C at a rate of 10 °C/min. The final temperature was maintained for 2 min. The nitrogen flow rate (inert and sweep gas) was 75 ml/min. The first derivative of the weight loss as a function of time (DTG) was calculated from the weight loss on a dry basis. TG analysis was performed for three parts (base, middle and top branches) of each crude hybrid, hybrid without extractives and structural components (holocellulose, cellulose and lignin).

2.5. Fourier transform infrared (FTIR) spectroscopy

FTIR measurements were carried out on a Nicolet IR 8700 spectrometer fitted with a highly sensitive mercury-cadmium telluride detector (MCT-A) operating at sub-ambient temperature and a Smart Collector diffuse reflectance (DRIFT) accessory. Spectra of the dried samples were obtained by co-adding 64 scans with a resolution of 4 cm^{-1} over the range 4000–650 cm^{-1}. Several FTIR indices comparing the maximum intensities (I) of selected absorption bands were used to evaluate the changes in the chemical structure of the raw samples.

3. Results and discussion

Morphological traits of the three parts (top, middle and base) of the four types of hybrid poplars reveal that bark thickness increases with average wood diameter, which is why it is higher in the base of the trees (2.06–4.56 mm), followed by the middle part (0.82–3.18 mm) and the top branches (0.82–1.19 mm) (Table 1). However, bark thickness is not only related to the wood diameter but also the species of poplar and the tree age affect the anatomical features. In contrast to bark thickness, the highest bark content (bark weight with respect to that of the whole section, including wood and bark) is sited in the upper section of the trees because the proportion of wood/bark by weight increases from the top to the base. The samples from Monviso, a 5-year short second-rotation poplar, are the ones with the highest bark content, and the inner wood/bark ratio by weight seems to be relatively constant along the tree. These features before harvesting directly affect the biomass quality and economic value as energy source and feedstock.

3.1. Chemical and lignocellulosic composition of the hybrid poplars

Regarding proximate and ultimate parameters and heating values -high and low heating values (HHV and LHV, respectively)- data are relatively similar for all the samples (Table 2). Wood samples are characterized by high volatile matter (80.58–83.78 wt% db) and low ash contents (0.51–1.14 wt% db), resulting in low fixed carbon (15.60–18.35 wt% db) compared with peat and low-rank coals such as lignite (with averages of 38 and 46 wt% db, respectively [23]). Accordingly, the C contents (49.13–51.67 wt% db) of the samples are low, whereas their O contents (40.63–43.87 wt% db) are high because the samples have not undergone a coalification process. During coalification, the organic matter of biomass increases its carbon content and decreases its oxygen content giving rise to the carbon-enriched structure of coal. The lack of biochemical and/or geochemical transformations is also linked to their low heating values, but similar to peat and lignite, 18.56 and 19.05 MJ/kg, respectively, due to the high volatile matter.

Cell wall components of hybrid poplars that contribute to the physico-chemical properties include the three natural biopolymers -cellulose (39.4–54.0 wt% db), hemicellulose (19.8–26.9 wt% db) and lignin (19.0–25.6 wt% db)- together with non-structural components (extractives and minerals) in various amounts (Table 3). Beaupré hybrid -a 9-year short first-rotation poplar- is the one that shows higher cellulose content. Relationships between hemicellulose contents and the section or the age of trees were not found.

As shown in Table 3, there is a remarkable similarity in the physico-

Table 1
Some anatomical features of the samples from the hybrid poplars.

Genotype	AF2			Beaupré			I214			Monviso		
Taxon	*Populus x canadensis*			*Populus x generosa*			*Populus x canadensis*			*Populus* × *generosa* × *Populus nigra*		
Parent species	*P. deltoides x P. nigra*			*P. deltoides x P. trichocarpa*			*P. deltoides x P. nigra*			*P. trichocarpa x P. deltoides x P. nigra*		
Rotation cycle	2			1			1			2		
Age in years	5			9			8			5		
Tree part	T	M	B	T	M	B	T	M	B	T	M	B
Total moisture (wt%)	53	56	51	26	55	49	24	60	44	30	53	49
Bark thickness (mm)	1.19	3.18	3.87	0.82	1.40	2.15	1.04	1.80	4.56	1.03	0.82	2.06
Wood diameter (mm)	24.2	55.6	89.3	23.0	41.8	56.0	25.3	69.3	110	17.8	41.5	60.0
Bark (wt%)	22.3	20.6	14.9	19.9	11.9	11.8	22.3	14.1	11.5	24.6	21.4	23.8
Wood/bark weight ratio	3.48	3.85	5.71	4.03	7.40	7.47	3.48	6.09	7.70	3.07	3.67	3.20

Data of AF2, Beaupré and I214 samples were reported in [12].

Table 2
Chemical characteristics and calorific value of the hybrid poplars.

Genotype	AF2			Beaupré			I214			Monviso		
Tree part	T	M	B	T	M	B	T	M	B	T	M	B
Moisture (wt%)	4.73	4.48	4.07	4.53	5.00	4.14	5.74	4.87	3.94	4.89	5.01	3.55
Ash at 815 °C (wt% db)	1.03	0.87	0.85	1.06	0.62	0.68	1.14	0.75	0.51	1.07	0.83	0.86
Ash at 550 °C (wt% db)	1.80	1.52	1.55	1.66	1.25	1.35	2.26	1.43	1.10	2.31	1.38	1.12
Volatile matter (wt% db)	80.85	81.00	81.82	81.88	83.78	83.72	80.95	81.52	82.06	80.58	81.79	82.16
Fixed carbon (wt% db)	18.12	18.13	17.33	17.06	15.60	15.60	17.91	17.73	17.43	18.35	17.38	16.98
C (wt% db)	50.31	50.53	49.72	49.32	49.59	49.13	50.15	50.24	49.75	51.67	49.88	49.79
H (wt% db)	5.98	5.97	6.04	6.14	5.97	6.01	6.08	6.02	6.01	6.08	6.03	6.11
N (wt% db)	0.65	0.42	0.35	0.47	0.33	0.30	0.77	0.45	0.35	0.53	0.33	0.29
S (wt% db)	0.03	0.02	0.01	0.02	0.01	0.01	0.02	0.02	0.01	0.02	0.02	0.01
O_{dif} (wt% db)	42.00	42.19	43.03	42.99	43.48	43.87	41.84	42.52	43.37	40.63	42.91	42.94
HHV (MJ/kg)	19.96	19.89	19.74	19.79	19.64	19.53	19.96	19.93	19.65	19.95	19.94	19.47
LHV (MJ/kg)	18.74	18.67	18.50	18.53	18.42	18.30	18.72	18.70	18.42	18.71	18.70	18.21

Proximate and ultimate analysis of AF2, Beaupré and I214 samples were reported in [12].

Table 3
Structural components and extractives of the hybrid poplars (data are normalized to 100%).

Genotype	AF2			Beaupré			I214			Monviso		
Tree part	T	M	B	T	M	B	T	M	B	T	M	B
Cellulose (wt% db)	39.43	45.10	42.78	46.90	53.86	54.05	45.20	47.71	49.90	44.64	48.07	49.94
Hemicellulose (wt% db)	23.67	22.87	26.90	21.76	19.80	21.49	22.47	25.82	22.82	20.59	22.45	24.48
Lignin[a] (wt% db)	24.06	23.91	23.79	20.66	20.50	18.97	24.64	23.39	23.60	25.62	23.03	19.31
Total Extractives (wt% db)	12.84	8.12	6.52	10.67	5.85	5.49	7.69	3.07	3.69	9.15	6.44	6.28
E_{water} (wt% db)	8.82	6.01	5.08	8.92	4.49	3.87	6.73	2.97	3.66	7.40	5.60	4.87
$E_{acetone}$ (wt% db)	4.02	2.11	1.44	1.75	1.36	1.61	0.96	0.10	0.03	1.75	0.84	1.40

[a] Acid-insoluble lignin by Klason method

chemical features of the samples. However, the relative proportion of components shows noticeable height-related changes. For cellulose content, the absolute values of the relative deviations for the top samples with respect to that of the corresponding tree base are 8%, 13%, 9% and 10% in AF2, Beaupré, I214 and Monviso, respectively. For hemicellulose and lignin contents, they are 12% and 1%, 1% and 9%, 2% and 4% and 16% and 33%, respectively. Except for hemicellulose content in Beaupré, the relative deviations are higher than the standard deviations found in the replicated determinations (0.1%, 1.5% and 0.07% for cellulose, hemicellulose and lignin, respectively). For this complex biopolymer, there is an apparent increase in content from the base to the top of the trees, related to bark content [12]. The biopolymers such as hemicellulose and lignin join the different layers of cell walls located between cellulose fibers [10], and higher contents imply higher physical and chemical energies for separating these layers.

In addition to the main structural components of the cell wall, wood contains many organic and inorganic non-structural substances known as extractives with a wide degree of solubility in water and different organic solvents. The amount and composition of wood extracts varies widely in different wood species, and the growing conditions and tree age also play an important role in wood utilization.

Total extractives range between 7.7 and 12.8 wt% db, 3.1–8.1 wt% db and 3.7–6.5 wt% db for the top, the middle and the base of the hybrids, respectively. In general, for lignocellulosic biomass, this content varies from 3 to 15 wt% [24,25]. Extractive content is higher in young hybrids with a higher heartwood proportion than in older specimens. Monviso and AF2, the youngest poplars (5 years), have the highest bark contents. Klasnja et al. [26] indicated that the proportion of bark decreases with age for the specimens studied (poplar and willow clones). In the set of samples studied, the bark content cannot be *per se* used as a clear marker of high or low lignin content. However, in general, the younger the tree or its section (upper sections), the higher the bark content and, consequently, the higher the lignin and extractive contents. The increase in both is related to the fact that bark is rich in lipophilic extractives and aromatic compounds, including tannins and lignin [27]. Meszaros et al. [8] also found that young wood barks contain more extractives than older ones. They also reported significantly higher inorganic contents in bark than in wood. On the other hand, slight increases in N and S contents, ash yield and HHV can be observed at the higher up the tree the sample was taken from (Table 2). However, proximate analysis and HHV depend on other aspects, such as poplar genotypes. González-González et al. [28] found higher N concentrations in I214 than in Monviso and AF2 in poor water conditions and under Mediterranean climatic conditions. I214 was the genotype with the highest N contents (Table 2).

As regards the solvent used for extraction, there is a dominance of the fraction extracted with hot water that constitutes from nearly 70–99% of the total extractives, with the rest corresponding to lipophilic compounds extracted with acetone.

3.2. Structural features of the hybrid poplars

The DRIFT spectra of the raw samples are shown in Fig. S2. All the spectra are characterized by features common to biomass components that can be attributed to a specific cell-wall biopolymer [29,30] a strong and broad hydrogen-bonded O-H stretching around 3420 cm^{-1} and a composite band of C-H aliphatic stretching vibrations at 2920 cm^{-1} accompanied by the corresponding CH_2 bending vibrations at 1458 cm^{-1}, polysaccharides being the major contributors to these bands; a prominent band centered at about 1740 cm^{-1} attributed to C=O stretching modes in non-conjugated systems of hemicellulose structure and at nearly 1655 cm^{-1} attributed to O-H absorbed and C=O functionalities in conjugated systems; νC=C bands at 1596 and 1506 cm^{-1} of aryl rings in phenolic systems characteristic of lignin, whose relative intensity is dependent on the lignin maturity; alkyl C-H bending modes near 1375 cm^{-1}attributed to methyl groups; and other additional bands in the 1300–1000 cm^{-1} region of the contributions of various C-O vibration modes in carbohydrates and lignin.

In addition to the main absorption bands, one minor and weak absorption can be observed at 898 cm^{-1}. This band arises purely due to C-H deformation in the amorphous region of cellulose [31] and may be used as a marker band for cellulose.

From the source-specific spectral bands and their intensity, some FTIR indices defined as the ratio of the absorbance intensity of selected bands can be used for diagnostic purposes (Table 4). The absorption bands were selected because they refer to only one cell-wall biopolymer. Thus, the bands at 1596 and 1506 cm^{-1} are associated with lignin [32], while 898 cm^{-1} to amorphous cellulose regions [31]. The I_{1596}/I_{1506} index reflects differences in the aromatic C═C environment of lignin and represents spectral signatures of lignin maturity [29]. All the samples have an index near unity, and the common features between tree sections are the highest ratio for the base and the lowest ones for the middle of the tree. An I_{1596}/I_{1506} index higher than unity indicates a high amount of aromatic C═C bonds absorbing close to 1596 cm^{-1}, reflecting a sort of lignin maturity at the tree base.

The other two indices, I_{1596}/I_{898} and I_{1506}/I_{898}, also allow the different raw samples to be distinguished [12], decreasing when moving from the top to the base of the trees and suggesting an increase in cellulose.

3.3. Pyrolysis profiles of the hybrid poplars

The distribution of woody biomass components on the pyrolytic thermal behaviour can be evaluated by TG analysis. Fig. 1 shows the pyrolysis DTG profiles of the three sections (top, middle and base) from the four hybrid poplars, as well as those of their isolated holocellulose and cellulose. All the profiles of the whole samples are very similar with a thermogravimetric pattern typical of hardwoods [29], showing a decomposition peak at around 350 °C (342–358 °C, Table S2) and two shoulders around 250 °C and 300 °C. The shoulder at 250 °C is more evident, even transforming into a peak, for the top samples of the trees.

During the temperature interval 120–250 °C, the mass loss ranges between 4.2 and 8.1 wt%, which can be attributed to the onset degradation of extractives, hemicellulose and thermally unstable lignin [29, 33]. Hemicellulose seems to begin decomposition at around 200 °C since the DTGs of holocellulose and those of the whole samples from 200 °C to 270 °C are nearly coincident for the majority of the samples. Thus, extractives seem not to play a significant role in middle and base pieces in this temperature interval. The highest devolatilization percentages correspond to the top section of the trees. For these samples, a small peak with a maximum decomposition rate at about 220 °C can be seen (Fig. 1). These peaks disappear when extractives are removed, which indicates that they are related to some extractive component degradation and/or their effect on lignin decomposition. The same finding was observed by Sebio-Puñal et al. [34] for *Pinus pinaster* pyrolysis. Between 250 and 300 °C, the mass losses (14.9–15.9 wt%) are predominantly due to hemicellulose decomposition, although this will be significant until approximately 350 °C [29,35]. The mass loss in this temperature interval is much more uniform than that produced between 120 and 200 ºC, which agrees with the variability of extractive and lignin contents and the uniformity in hemicellulose content. The next event at 300–400 °C is mainly attributed to cellulose decomposition and exhibits the maximum volatile matter release in the range 342–358 °C (T_{max}), DTG$_{max}$ between 14.8% and 21.1%/min and 46.1–55.3 wt% of the total amount of volatile matter evolved (Table S3). There is some overlap with the end of hemicellulose degradation and significant breakdown of lignin. From 400–800 °C (mass-losses range between 7.5 and 11.1 wt%), still, the three structural components devolatilize, lignin showing the highest weight-loss rates. Small quantities of extractives, hemicellulose and cellulose may also contribute to the release of volatile matter. Additionally, inorganic species can be transformed at high temperatures, releasing volatile species. Although ash yield is low (<1.2 wt% db), inorganic species may have a significant catalytic effect [36]. Generally, the upper parts of the trees show slightly higher mass loss percentages for this temperature interval, which agrees with the fact that this younger section contains more lignin and extractives.

Table 4
FTIR indices of the different samples and their significance.

Index significance	Lignin maturity	νC═C (lignin)/γCH (cellulose)	νC═C (lignin)/γCH (cellulose)
FTIR index	I_{1596}/I_{1506}	I_{1596}/I_{898}	I_{1506}/I_{898}
AF2-T	1.013	6.684	6.601
AF2-M	0.962	6.268	6.519
AF2-B	1.105	5.984	4.846
Beaupré -T	0.987	6.411	6.498
Beaupré -M	0.902	4.766	5.286
Beaupré -B	1.067	4.606	4.317
I214-T	0.987	7.148	7.245
I214-M	0.952	5.657	5.945
I214-B	1.005	4.715	4.689
Monviso-T	1.060	6.261	5.910
Monviso-M	1.046	6.246	5.967
Monviso-B	1.252	5.191	4.148

Table S2 reflects the main characteristic parameters of the thermogravimetric curves of the hybrid poplars: (i) maximum rate of decomposition (DTG$_{max}$) and its associated temperature (T_{max}); (ii) mass loss percentage up to T_{max} of the dried samples (X at DTG$_{max}$); (iii) initial and final decomposition temperatures (T_5 and T_{95} at conversion degrees of 5% and 95%, respectively); (iv) pyrolysis temperature interval (T_{95}-T_5); and (v) char yields at 500 °C and 800 °C (CY500 and CY800). The temperatures associated with a 5% conversion are lower for the top samples. On the other hand, for each type of hybrid, the tighter decomposition intervals (T_{95}-T_5) and the highest DTG$_{max}$ always occur for the middle sections.

3.4. Pyrolysis of extracted cellulose from the hybrid poplars

Fig. 1 shows the DTG profiles of the cellulose and holocellulose from the twelve samples. Table S3 summarizes the characteristic parameters of cellulose thermal degradation. Cellulose decomposes in a narrow temperature range (T_{95}-T_5), starting around 286 °C and ending in the 377–499 °C range with the lowest temperature for the I214 base (age: 8-years) and the highest for the Beaupré base (age: 9-years). T_{max} values are comprised in a tight interval of 322–338 °C. The values are lower than those reported by Chen et al. [37] for poplar cellulose (361.4 °C) due to a higher heating rate (15 °C/min) than in this work (10 °C/min) and differences in crystallinity. However, the pyrolysis of isolated cellulose can show differences concerning its behaviour when it remains unaltered in the whole sample. Differences can be attributed to opposite effects on the thermal stability of isolated cellulose: (i) the lost and/or weakening of some H bonds (associated with crystallinity reduction) because of delignification by the Wise method [38] (a reduction); (ii) the removal of its links with lignin (a reduction); and (iii) the removal of the catalytic effect of some inorganics in extractives (an increase). Higher thermal stability of cellulose is associated with a more robust and well-structured hydrogen bonding net that preserves the β-D-glucose ring structure during pyrolysis [39]. Thus, lower crystallinity is related to less thermal stability (earlier decomposition and lower activation energy), but a lower mass loss after pyrolysis and, consequently, a higher char yield [39]. Fig. 1 shows that, for these samples, the lost and/or weakening of some H bonds in cellulose and the effect of removing cellulose links with lignin have more influence than the elimination of extractives. Thus, compared with cellulose in the unaltered samples, isolated cellulose reaches much higher DTG$_{max}$ at lower temperatures (ΔT_{max} ranges 12 °C – 32 °C) and its decomposition finishes before. Similar behaviour can be observed for holocellulose pyrolysis.

3.5. Pyrolysis of extracted lignin from the hybrid poplars

Fig. 2 shows the pyrolysis DTG profiles of the isolated lignin, and Table S4 summarises their most relevant thermogravimetric parameters.

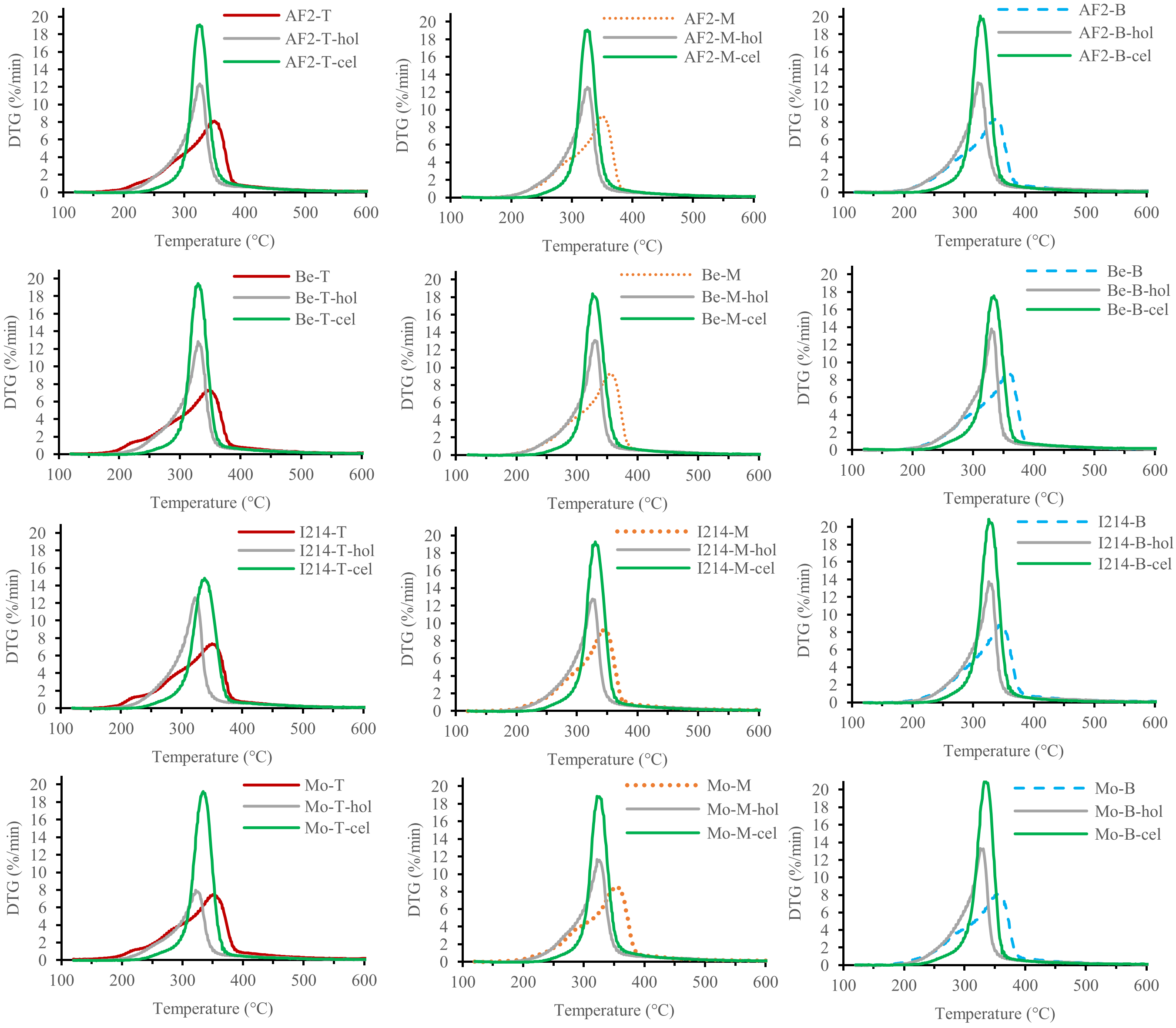

Fig. 1. Whole samples, holocellulose (hol) and cellulose (cel) DTGs of the top (T), middle (M) and base (B) of AF2, Beaupré (Be), I214 and Monviso (Mo).

Lignin is a complex and highly variable co-polymer derived from three monomers (monolignols) with different degrees of methoxylation: p-coumaryl, coniferyl and sinapyl alcohols [40]. Several typical inter-unit linkages in lignin can be found, comprising C-O and C-C bonds. Among C-O bonds, the β-O-4 sub-structure is the most abundant since it is present in 46–60% of the lignin linkages, depending on the type of biomass [41]. Its abundance plays a significant role in its properties, thermal stability, and pyrolytic cleavage mechanisms [42]. Moreover, the biomass treatments for extracting lignin affect lignin structure. During Klason treatment (used in this research), fragmentation of β-O-4 linkages together with condensation reactions, in which phenolic hydroxyl groups participate, occurs [42]. Thus, the lignin extracted from the samples after the removal of extractives has a higher condensation degree than in the non-treated materials, contains fewer methoxy groups, can be converted into char more efficiently and is more thermally stable. Nevertheless, the condensation degree of the Klason lignin depends on the original lignin structure in the samples.

The temperature interval for lignin decomposition (T_{95}-T_5) is broader than for cellulose (Table S4). A conversion degree of 5% is reached at a temperature in the range of 246–281 °C (lower temperatures than those of cellulose), whereas at a temperature between 627 and 761 °C (higher temperatures than those of cellulose), the 95 wt % loss is produced (Table S4).

In the pyrolysis DTG profiles of the lignin of the twelve samples (Fig. 2), the following intervals can be distinguished: 200–300 °C, 300–400 °C, 400–500 °C and 500–800 °C. From 200–300 °C, a small shoulder associated with a mass loss of around 4 wt% can be observed. Cleavage of the weakest C-O bonds in the β-O-4 structure occurs between 150 and 350 °C [41,43] and is essential for the radical initiation reactions during pyrolysis [41]. Probably, in this interval, the methyl break of the methoxy groups also begins as its binding energy in the lignin structure is only slightly higher than that of β-O-4 linkage. Breaking a C-O bond cleavage requires less energy than a C-C bond [41].

In the 300–400 °C interval, the maximum weight loss (around 20–30%) and mass loss rate occur. In this temperature interval, the methyl cleavage of the methoxy groups is very significant. This may be supported by the large quantity of CH_4 production reported during lignin slow-pyrolysis in the range of 300–650 °C, with a maximum at around 400 °C [44,45]. Additionally, some side-chain hydroxyl groups may undergo cleavage. This agrees with the reported CH_3OH formation

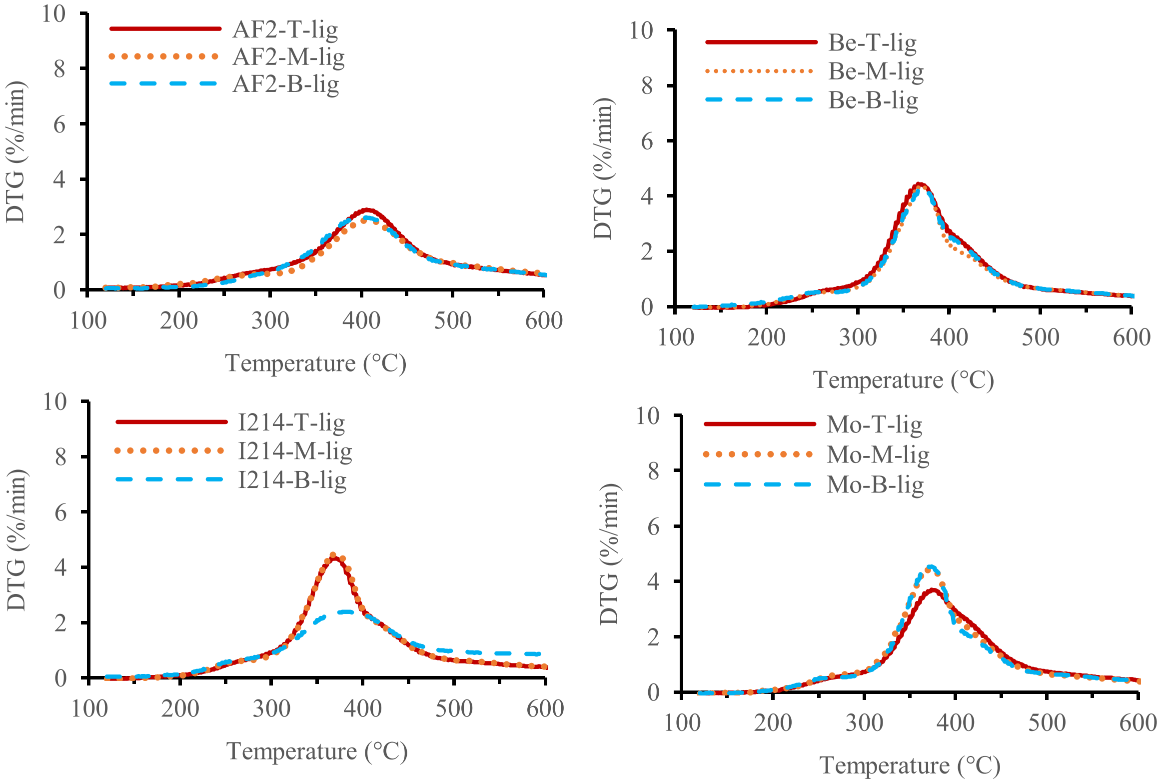

Fig. 2. Lignin (lig) DTGs of the top (T), middle (M) and base (B) of AF2, Beaupré (Be), I214 and Monviso (Mo).

from lignin pyrolysis in the 300–450 °C range [44]. Hydroxyl radicals are more reactive than phenoxy and alkyl ones [28].

The abundance of methoxy groups is related to the relative quantities of Guaiacyl (G), Syringyl (S) and p-hydroxyphenyl (H) units in lignin. As these work samples can be classified as hardwood type, their lignin is characterized by G and S units, and only traces of H-units can be expected. Thus, until 400 °C, mainly S-type-lignin (less stable) may predominantly decompose, whereas G-type-lignin decomposition becomes more relevant at higher temperatures. During pyrolysis, S units demethoxylation is more accessible than that of the G units [46], especially at temperatures lower than 400 °C. Yokoi et al. [47] noted a decreasing trend in G/S ratios from the base to the top of the tree they studied. The presence of more β-O-4 linkages in the lignin structure (lower G/S ratio) [46], which means a lower condensation degree in lignin structure, may be related to the hybrid youth and health. Thus, the healthier and younger the tree, the more C-O bonds exist, accelerating decomposition during pyrolysis.

Between 400 and 470 °C, all the samples except for I214-base and AF2 (T, M and B) show a shoulder. This may be mainly associated with hydroxyl and methoxy elimination. Chu et al. [41] suggested that solid products from pyrolysis at 550 °C still contain hydroxyl groups.

During 470–800 °C, re-polymerization produces a polyaromatic char. Mass loss at this stage may be associated with char reduction and the water gas shift reaction with CO_2 being generated in significant amounts from 600 to 800 °C [41,44,45].

3.6. *Effect of lignin removal on the thermal stability of holocellulose and cellulose*

Fig. 3 shows the experimentally pyrolysis DTG profiles of the samples without extractives (DTG_{free}) and holocellulose, and the calculated ones from the DTG of the isolated lignin and holocellulose, considering their proportions in the samples ($DTG_{free\text{-}cal}$). Without interactions between lignin and holocellulose and alterations produced by component isolation processes, DTG_{free} and $DTG_{free\text{-}cal}$ should be approximately coincident. However, significant differences can be observed for $DTG_{free\text{-}cal}$: (i) the main decomposition takes place in a tighter range and at lower temperatures, and (ii) T_{max} shifts to lower values (around 45 °C before).

$DTG_{free\text{-}cal}$ and those of holocellulose are similar (Fig. 3) because the percentage of lignin is significantly lower, its decomposition rate is much lower than that of hemicellulose, and it is thermally more stable. Thus, the above differences between $DTG_{free\text{-}cal}$ and DTG_{free} can be attributed to an apparent reduction in the thermal stability of holocellulose. As mentioned, delignification by the Wise method reduces cellulose crystallinity. However, Leng et al. [39] compared the pyrolysis profiles of crystalline and amorphous cellulose and found that the DTG_{max} of amorphous cellulose is higher than that of crystalline cellulose. Moreover, for amorphous cellulose, there is a shift in the peak temperature (ΔT_{max}) of 5 °C towards higher temperatures [39]. In contrast, in the DTG of holocellulose and $DTG_{free\text{-}cal}$ (both have cellulose with lower crystallinity than DTG_{free}), ΔT_{max} (towards lower temperatures) ranges from 39 °C to 52 °C, which indicates that the reduction in thermal stability of $DTG_{free\text{-}cal}$ and holocellulose is not due mostly to cellulose alteration in the delignification process. It can be mainly associated with the breakage of cellulose/lignin and hemicellulose/lignin bonds because of carbohydrate separation. This fact is related to wood structure characteristics in which lignin fibers reinforce cellulose and hemicellulose [9]. A positive relationship exists between ΔT_{max} and lignin content ($r^2 = 0.62$), which reinforces the hypothesis that carbohydrate/lignin bond breakage is the key factor in the above thermal stability reduction.

In DTG_{free} compared to $DTG_{free\text{-}cal}$, there seems to be a more noticeable difference between hemicellulose and cellulose pyrolysis. In DTG_{free}, hemicellulose decomposition seems to finish at around 350 °C and, from this temperature, the decomposition rate increases sharply until reaching the peak temperature. This drastic acceleration may be due to the lack of all the β-O-4 linkages of lignin and the connections between hemicellulose and lignin (hydrogen and covalent bonds [48]). Afterward, the cleavage of H bonds between cellulose and lignin would be easier and, consequently, faster. This agrees with the shapes of

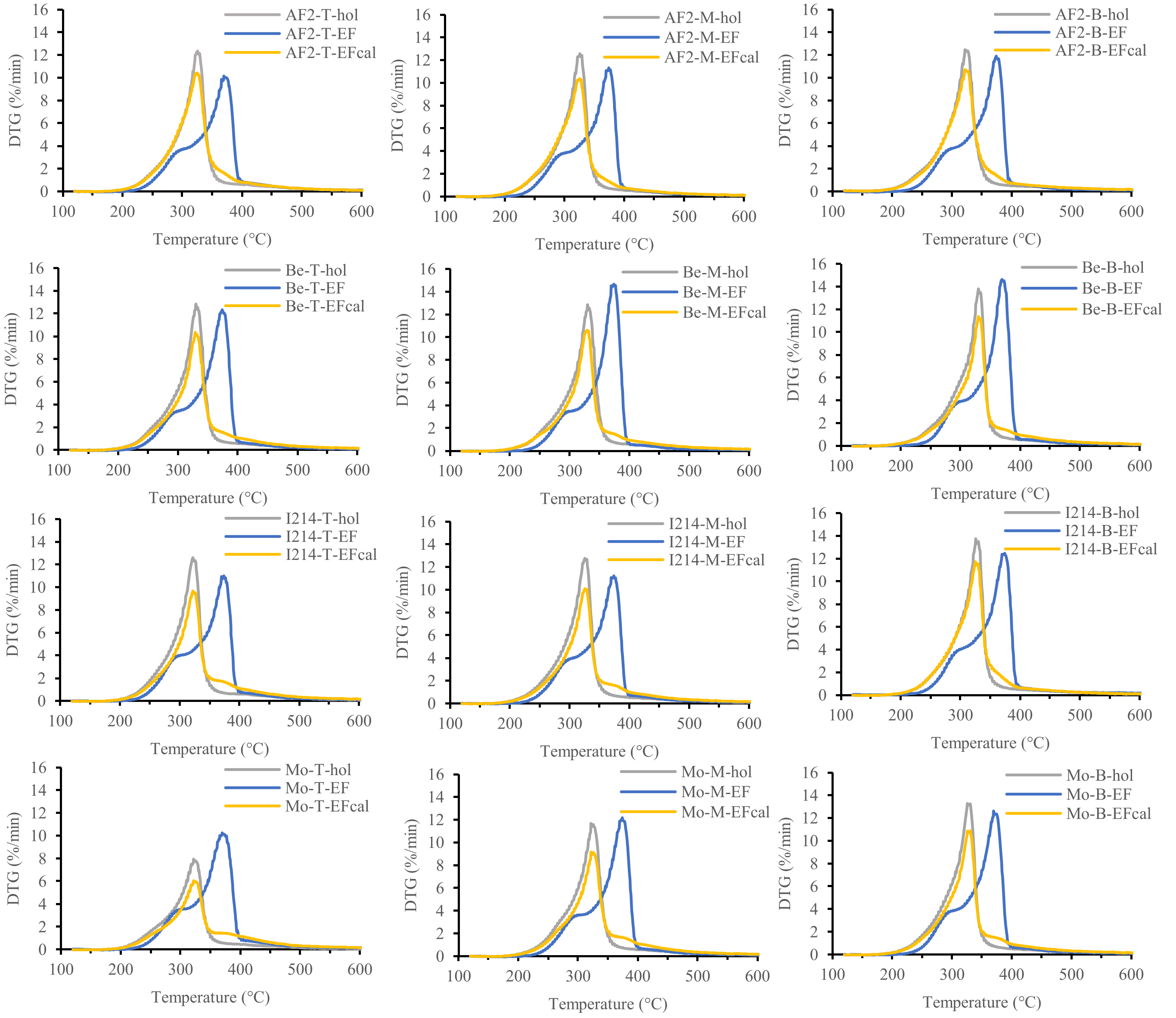

Fig. 3. DTGs of holocellulose (hol) and the samples without extractives (EF) and those calculated from the isolated components (holocellulose + lignin) (EFcal).

DTG_{free} from 350 °C are very similar to those of $DTG_{free\text{-}cal}$ from 270 °C, but the formers evolve at higher temperatures. Therefore, lignin has a clear protection link effect that gives cohesion, strength, and thermal stability to the cell wall structure. The tight relationship between lignin and hemicellulose seems to be related to the reported difficulty in breaking the complex lignin-carbohydrate structure in the lignin isolation process [15].

3.7. *Effect of extractives on the thermal stability of the samples*

Extractives comprise a wide variety of substances and, according to their water solubility, they can be classified into two categories (hydrophilic and hydrophobic extractives). Hydrophilic compounds, soluble in high-polarity solvents, are mainly phenolic compounds (flavonoids and non-flavonoids). They have antioxidant properties and are mainly present in leaves and bark, whereas hydrophobic compounds that are soluble in low-polarity solvents include terpenes and free or esterified fatty acids [49].

In Fig. 4, pyrolysis profiles of the un-extracted poplars (DTG_{raw}) compared to those without extractives (DTG_{free}) can be seen. The hybrids contain higher extractives soluble in hot water than in acetone (Table 3). In general, the higher the position the sample was taken from (younger section), the higher the water-soluble extractive content.

By comparing both profiles (DTG_{raw} and DTG_{free}), the following effects because of extractive removal can be seen: (i) T_{max} moves to higher temperatures, the shift being in the 12–32 °C interval (Tables S2 and S5) and, (ii) there is an increase in the maximum rate of decomposition (DTG_{max}) comprised in the interval 2.0–5.8%/min. In general, the lower the position of the sample in the tree (more cellulose), the higher the ΔDTG_{max}

Although the shoulder at around 250 °C disappears (it only exists in the un-extracted samples from the top), the one at approximately 300 °C does not. Thus, up to about 270 °C, DTG_{raw} (associated with hemicellulose, extractives and lignin decomposition) is relatively similar to that of holocellulose but shows slightly higher decomposition rates than DTG_{free} (Fig. 4). The differences can be attributed to the removal not only of the extractives, but also of low-molecular polysaccharides inevitably subtracted [17]. From 270–350 °C, the evolution of both profiles is nearly parallel, with DTG_{free} showing lower weight loss rates. This may be related to the fact that the extraction with solvents removes

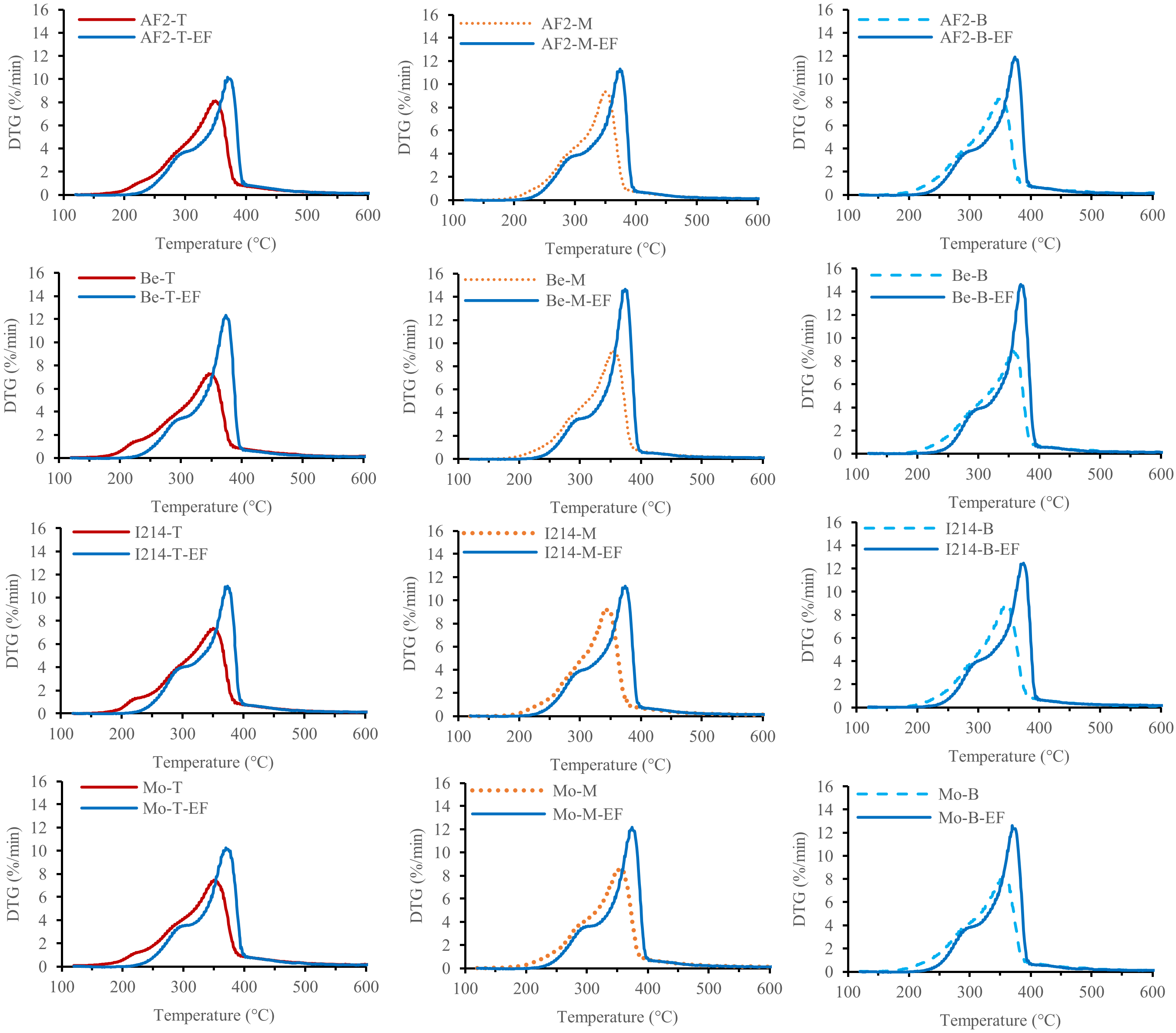

Fig. 4. DTGs of the whole samples (un-extracted samples) and those without extractives (EF).

inorganic matter that may catalyze organic matter degradation [17]. Table S6 shows the ash contents of the raw and extractive-free samples, experimentally and estimated ones, and the ash distribution between insoluble and soluble fractions from the extraction process. For all the samples, the ash distribution between insoluble and soluble-extraction fractions indicates a high degree of solubilization of some mineral species during extraction processes. The solubilization and retention levels depend on the tree specie and the position of the sample in the tree. The elementary ash microanalysis by EDX reveals dominance of Ca and K in ashes, with other elements such as Na, Mg, P, Al, Si and S. Ca-mineral species such as Ca element and carbonates are present as finely dispersed small particles and embedded within discrete areas of other mineral species. Fig. S3 shows, as an example, some microphotographs, spectra and composition of selected areas and spots, showing the abundance of Ca and K in the samples.

From 350 °C and for DTG_{free}, thermal degradation is accelerated, a peak with a higher maximum rate than DTG_{raw} being reached. This peak is due to lignin and a significant portion of cellulose degradation, and its T_{max} is very similar to that of isolated lignin.

However, when the structural components have not been previously extracted, the T_{max} of DTG may be associated with the simultaneous massive decomposition of cellulose and lignin (after the cleavage of β-O-4 linkages and hemicellulose/lignin connections), which occurs at approximately 350 °C (with extractives). When extractives are removed, the main simultaneous decomposition of cellulose and lignin occurs at a higher temperature in a very tight interval and at a higher DTG_{max}, approximately equal to that of isolated lignin. The extractive removal seems to affect cellulose and lignin more than hemicellulose, which agrees with the fact that hemicellulose remains more enriched in extractives after the treatment with solvents. Accordingly, Cagnon et al. [50] concluded that hemicellulose yields higher ash than other fractions, indicating higher inorganic matter concentration.

3.8. Relationships of proximate analysis and calorific value with lignocellulosic composition and chemical structure

Table 5 shows several multiple linear relationships that predict variables of proximate analysis and HHV as a function of lignocellulosic composition and/or FTIR indices. Fig. 5 shows the results of applying the correlations against experimental data. The correlations predict variable

Table 5
Relationships between different parameters of hybrid poplar characterization.

Eq. number	Equation	Correlation coefficient (R^2)	Sum of squared errors
1	$VM = 87.36 - 10.15 * (\text{lignin}/\text{cellulose}) - 0.182 * E_{water} + 0.302 * E_{acetone}$	0.830	1.97
2	$VM = 0.623 * \text{lignin} + 0.933 * \text{cellulose} + 0.792 * \text{hemicellulose} + 1.13 * E_{acetone} + 0.664 * E_{water}$	1.000	1.80
3	$Ash = -0.0266 * \text{lignin} + 0.250 * I_{1596}/I_{898}$	0.993	0.064
4	$Ash = 0.0095 * \text{lignin} + 0.190 * I_{1596}/I_{1506} + 0.078 * E_{water}$	0.988	0.110
5	$HHV = 18.85 + 0.165 * I_{1506}/I_{898}$	0.784	0.077
6	$HHV = 18.81 + 0.166 * I_{1506}/I_{898} + 0.027 * I_{1596}/I_{1506}$	0.783	0.077

All the variables of proximate analysis and lignocellulosic composition are expressed in (wt%, db) and HHV in MJ/kg. Contents of structural components and extractives are normalized to 100%.

values reasonably. All the points are within an interval calculated value ± 1.5 for volatile matter yield and a calculated value ± 0.2 for ash yield and HHV (dashed lines in Fig. 5). The first equation of Table 5 (Eq. 1) shows the relationship between volatile matter, lignin/cellulose ratio and extractive contents (water-soluble and acetone-soluble extractives). The independent coefficient (87.36 wt% db) of Eq. (1) is slightly higher than the mean value of volatile matter for all the samples (81.84 wt% db). Therefore, the independent variables modify volatile matter yield from its mean value. According to the multiple regression coefficients, the lignin/cellulose ratio is the variable with the most substantial influence, more than ten times higher than extractive contents. Additionally, the higher the lignin/cellulose ratio, the lower the volatile matter yield. The significant effect of this ratio on volatile matter yield in comparison with extractive contents and its negative relationship are in good agreement with the discussion of the previous sections. Thus, the link effect of lignin on cellulose (it increases with higher values of lignin/cellulose ratio) is more relevant to the wood thermal stability than extractive contents.

Eq. (2) shows the multiple linear regression between volatile matter yield, structural analysis, and extractive contents (Table 5). In contrast to Eq. (1), Eq. (2) does not have an independent coefficient. It shows that the decreasing influence of the main structural components is as follows: cellulose content > hemicellulose content > lignin content. It agrees with the increasing order of solid residue left by lignocellulosic component pyrolysis: lignin > hemicellulose > cellulose [35]. On the other hand, the positive relationship between E_{water} and volatile matter may be related to the inorganic content of E_{water} and the catalytic effect of these inorganics on organic matter degradation.

In contrast with volatile matter yield, for ash yield, the best correlations include FTIR indices as independent variables. This is probably because different types of lignin in samples do not affect volatile matter substantially due to the experimental conditions. However, the type of lignin (level of maturity) has a marked influence on ash yield. Table 5 shows two correlations for ash yield (Eqs. 3 and 4) that do not have independent coefficients. Eq. (3) indicates that the I_{1596}/I_{898} index is the

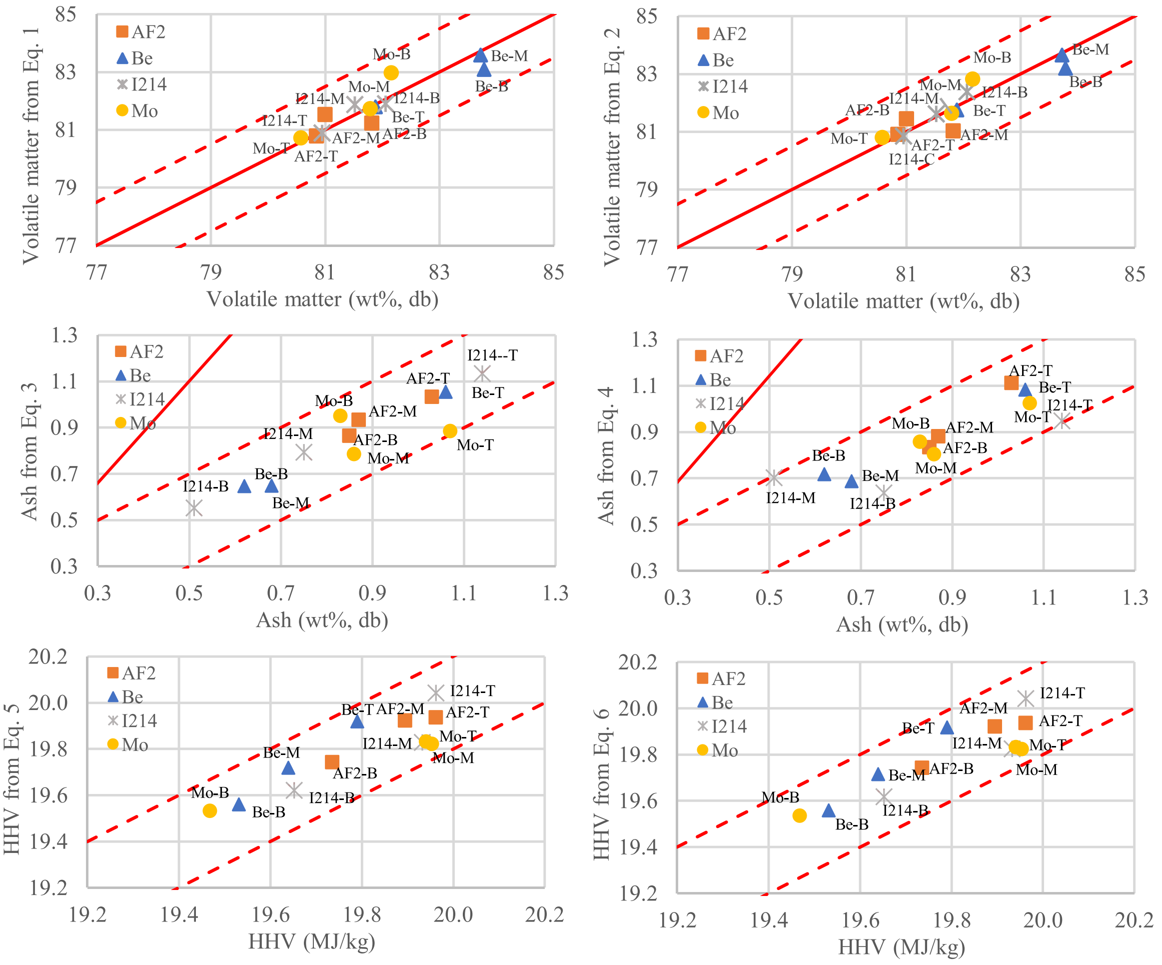

Fig. 5. Relationships between experimental data and those predicted from equations given in Table 5.

variable that affects ash yield the most. This index is the ratio of the heights of the marker bands 1596 cm^{-1} (characteristic of lignin and some types of extractives) and 898 cm^{-1} (characteristic of cellulose). The band at 1596 cm^{-1} represents C=C aromatic stretching vibrations, while the band at 898 cm^{-1} represents the C-H out-of-plane deformation of glucose rings in cellulose. The higher the index I_{1596}/I_{898}, the higher the ash yield. This is in good agreement with the fact that bark (more lignin) contains higher inorganics than wood [8]. Eq. (4) also shows the importance of lignin content in ash yield.

Additionally, in this equation, the I_{1596}/I_{1506} index is the most relevant variable, which suggests that distinguishing the chemical structure of lignin is a key factor for predicting ash yield. Thus, higher values of I_{1596} may be indicative of more G-type lignin content (higher relative content of C=C bonds and less oxygenated functional groups), which means more thermal stability of lignin. Then, for the same lignin content, if higher I_{1596}/I_{1506} values are associated with higher G-type lignin/S-type lignin ratios, they also imply higher ash yields. The samples from the base of the trees have higher values of the I_{1596}/I_{1506} index, which indicates that older sections (base) have more evolved lignin and higher G/S ratios (in accordance with Section 3.5 discussion).

Eq. (5) of Table 5 expresses HHV as a function of the I_{1506}/I_{898} index. Thus, similarly to ash yield, the types of lignin significantly affect HHV. The intercept of Eq. (5), which represents the HHV of cellulose and hemicellulose ($I_{1506}/I_{898} = 0$), is equal to 18.85 MJ/kg, a value similar to those of cellulose and hemicellulose [17]. The other term of Eq. (5) is a correction of cellulose and hemicellulose HHV that considers lignin HHV. I_{1506}/I_{898} is related to the ratio of *less evolved lignin/cellulose,* and its relationship with HHV is positive since the HHV of lignin is higher than those of cellulose and hemicellulose. Finally, Eq. (6) adds the I_{1596}/I_{1506} index to the correlation. This new term does not improve the fit but shows that the higher the I_{1596}/I_{1506} index, related to *more evolved lignin / less evolved lignin,* the higher the HHV.

Therefore, lignin content and maturity (or degree of evolution) are essential for predicting some properties of biomass as fuel. Lignin maturity is related to its chemical structure; the higher its maturity, the higher the G/S ratio (more C=C and less C-O bonds and β-O-4 structures), which produces higher thermal stability. Fig. 6 summarizes and interrelates the main findings of this manuscript.

To evaluate the performance of the prediction equations based only on FTIR indices (Eqs. 5 and 6), validation is conducted using an external set of seven wood samples: six wood samples taken from different parts of two hybrid willows (top, middle and base) and one whole sample from a young Beaupré hybrid poplar (Fig. S4). The results obtained from the numerical solution were found to be in satisfactory agreement with the experimental HHV values. Only slight differences were found between the predicted HHV values and those experimentally determined (47–368 kJ/kg from Eq. 5 and 49–253 kJ/kg from Eq. 6). Although the mathematical equations for HHV prediction were successfully validated with the current wood samples, future research needs to examine whether a universal equation is feasible.

DRIFT spectroscopy offers a simple and helpful tool for evaluating thermal properties of biomass.

4. Conclusions

Wood from three different heights (base, middle and top) of four types of hybrid poplars was evaluated. The extractive contents, chemical and structural compositions of the SRC poplars, and the pyrolytic behaviour of raw samples and structural components were obtained. For the highest sections (youngest ones) compared with those at lower positions, bark content increases, implying higher lignin content, fixed carbon and ash yields, and HHV. Also, they have more N, S and extractives. The latter is related to higher ash yield. Their lignin with more C-O (more β-O-4 structures) and less C=C bonds is less thermally stable. This type of lignin with a lower G/S ratio can be qualified as less mature.

Lignin has shown to be a key component for several reasons: (i) its concentration and chemical structure varies substantially with tree height; (ii) it conditions other structural component decomposition during pyrolysis; (iii) its removal affects biomass pyrolysis more than extractive removal; and (iv) it can be an important factor for predicting biomass properties as fuel.

Regarding its influence on biomass pyrolysis, the effect of lignin on thermal stability is so significant that cellulose does not reach its maximum decomposition rate until the breakage of lignin β-O-4 linkages and hemicellulose/lignin connections has occurred. From the cleavage of these bonds, which seems to finish at around 350 °C, the thermal

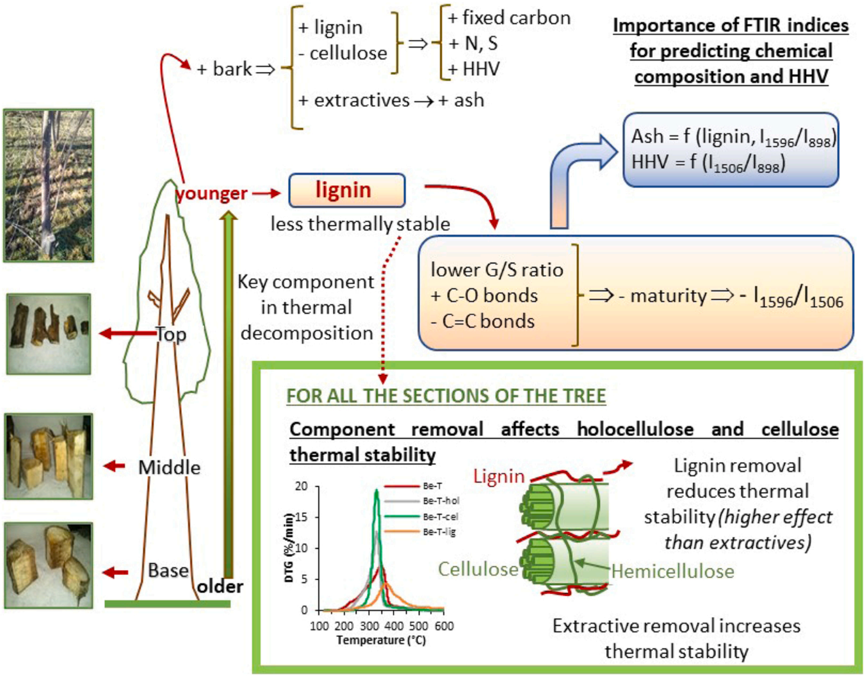

Fig. 6. Pyrolytic behaviour and variations of chemical and structural composition with tree height.

decomposition of the samples accelerates substantially, reaching a peak quickly.

Concerning the prediction of biomass properties as fuel, not only lignin content but also its chemical structure play important roles. Thus, for estimating ash yield and HHV of the samples at different heights of hybrid poplars, satisfactory relationships ($0.78 < r^2 < 0.99$) that use lignin and water-soluble extractive contents and FTIR indices as variables were obtained. Thus, the $I_{1596/1506}$ index is related to the abundance of aromatic C=C bonds in lignin and, subsequently, to the maturity of this biopolymer. The higher the above index, the higher the G/S ratio, which means higher lignin maturity and implies higher thermal stability. Therefore, since DRIFT spectroscopy can distinguish lignin structures, it is a helpful tool for evaluating differences in ash yield and HHV with tree height.

Declaration of Competing Interest

The authors declare that they have no known competing financial interests or personal relationships that could have appeared to influence the work reported in this paper.

Data Availability

No data was used for the research described in the article.

Acknowledgments

Funding from the Spanish National Research Council (CSIC) through the research project 202380E010 is gratefully acknowledged. The authors would like to thank the Doctors Pedro Álvarez Álvarez and Asunción Cámara Obregón of the Organisms and Systems Biology Department and María Castaño Díaz, University of Oviedo, Mieres Polytechnic School, Spain, for the supplier and assistance in collecting wood samples.

Appendix A. Supporting information

Supplementary data associated with this article can be found in the online version at doi:10.1016/j.jaap.2023.105861.

References

[1] M.W.H. Evangelou, H.M. Conesa, B.H. Robinson, R. Schulin, Biomass production on trace element–contaminated Land: a review, Environ. Eng. Sci. 29 (9) (2012), https://doi.org/10.1089/ees.2011.0428.

[2] N. Oliveira, R. Rodríguez-Soalleiro, C. Pérez-Cruzado, I. Cañellas, H. Sixto, R. Ceulemans, Above- and below-ground carbon accumulation and biomass allocation in poplar short rotation plantations under Mediterranean conditions, For. Ecol. Manag. 428 (2018) 57–65, https://doi.org/10.1016/j.foreco.2018.06.031.

[3] D.J. Daniel, C.R. Ellison, J. Bursavich, M. Benbow, C. Favrot, M.A. Blazier, C. Marculescu, S.E. Nokes, D. Boldor, An evaluative comparison of lignocellulosic pyrolysis products derived from various parts of *Populus deltoides* trees and *Panicum virgatum* grass in an inductively heated reactor, Energy Convers. Manag. 171 (2018) 710–720, https://doi.org/10.1016/j.enconman.2018.06.026.

[4] I. Laureysens, J. Bogaert, R. Blust, R. Ceulemans, Biomass production of 17 poplar clones in a short-rotation coppice culture on a waste disposal site and its relation to soil characteristics, For. Ecol. Manag. 187 (2–3) (2004) 295–309, https://doi.org/10.1016/j.foreco.2003.07.005.

[5] T.R. Rao, A. Sharma, Pyrolysis rates of biomass materials, Energy 23 (1998) 973–978, https://doi.org/10.1016/S0360-5442(98)00037-1.

[6] K. Slopiecka, P. Bartocci, F. Fantozzi, Thermogravimetric analysis and kinetic study of poplar wood pyrolysis, Appl. Energy 97 (2012) 491–497, https://doi.org/10.1016/j.apenergy.2011.12.056.

[7] E. Meszaros, E. Jakab, G. Varhegyi, P. Szepesvary, B. Marosvolgyi, Comparative study of the thermal behavior of wood and bark of young shoots obtained from an energy plantation, J. Anal. Appl. Pyrolysis 72 (2004) 317–328, https://doi.org/10.1016/j.jaap.2004.07.009.

[8] E. Meszaros, G. Varhegyi, E. Jakab, B. Marosvölgyi, Thermogravimetric and reaction kinetic analysis of biomass samples from an energy plantation, Energy Fuels 18 (2004) 497–507, https://doi.org/10.1021/ef034030.

[9] F. Rego, A.P. Soares Dias, M. Casquilho, F.C. Rosa, A. Rodrigues, Pyrolysis kinetics of short rotation coppice poplar biomass, Energy 207 (2020), 118191, https://doi.org/10.1016/j.energy.2020.118191.

[10] S. Wang, G. Dai, H. Yang, Z. Luo, Lignocellulosic biomass pyrolysis mechanism: a state-of-the-art review, Prog. Energy Combust. Sci. 62 (2017) 33–86, https://doi.org/10.1016/j.pecs.2017.05.004.

[11] P. Álvarez-Álvarez, C. Pizarro, M. Barrio-Anta, A. Cámara-Obregón, J.L.M. Bueno, A. Álvarez, I. Gutiérrez, D.F.R.P. Burslem, Evaluation of tree species for biomass energy production in northwest Spain, Forests 9 (2018) 160, https://doi.org/10.3390/f9040160.

[12] J.M. Gómez, M. Castaño, A. Cámara, P. Álvarez, M.B. Folgueras, M.A.Diez On, chemical composition and pyrolytic behaviour of hybrid poplar energy crops from northern Spain, Energy Rep. 6 (2020) 764–769, https://doi.org/10.1016/j.egyr.2019.09.065.

[13] M.D. Chaves Arantes, P. Fernando Trugilho, J. Tarcísio Lima, A. de Cássia Oliveira Carneiro, E. Alves, M.C. Guerreiro, Longitudinal and radial variation of extractives and total lignin content in a clone of Eucalyptus grandis W. Hill ex Maiden x Eucalyptus urophylla. S.T. Blake, Cerne 17 (3) (2011) 283–291, https://doi.org/10.1590/S0104-77602011000300001.

[14] M. Palacka, P. Vician, M. Holubčík, J. Jandačka, The energy characteristics of different parts of the tree, Procedia Eng. 192 (2017) 654–658, https://doi.org/10.1016/j.proeng.2017.06.113.

[15] J.L. Wen, S.L. Sun, B.L. Xue, R.C. Sun, Structural elucidation of inhomogeneous lignins from bamboo, Int. J. Biol. Macromol. 77 (2015) 250–259, https://doi.org/10.1016/j.ijbiomac.2015.03.044.

[16] A.N. Shebani, A.J. van Reenen, M. Meincken, The effect of wood extractives on the thermal stability of different wood species, Thermochim. Acta 471 (2008) 43–50, https://doi.org/10.1016/j.tca.2008.02.020.

[17] R.H. White, Effect of lignin content and extractives on the higher heating value of wood, Wood Fiber Sci. 19 (4) (1987) 446–452.

[18] X.J. Guo, S.R. Wang, K.G. Wang, Q. Liu, Z.Y. Luo, Influence of extractives on mechanism of biomass pyrolysis, J. Fuel Chem. Technol. 38 (1) (2010) 42–46, https://doi.org/10.1016/S1872-5813(10)60019-9.

[19] M. Castaño-Díaz, E. Afif Khouri, M. Barrio-Anta, J. Menendez-Rodriguez, A. Cámara-Obregón, Crecimiento y producción de biomasa de cultivos energéticos con sauce, chopo y abedul en terrenos ociosos de minería en el Norte de España. 7º Congreso Forestal Español. Gestión del monte: servicios ambientales y bioeconomía. Sociedad Española de Ciencias Forestales (SECF), Plasencia, Cáceres, 2017, 7CFE01–133, 13p (in Spanish).

[20] S.A. Channiwala, P.P. Parikh, A unified correlation for estimating HHV of solid, liquid and gaseous fuels, Fuel 81 (2002) 1051–1063, https://doi.org/10.1016/S0016-2361(01)00131-4.

[21] W.F. DeGroot, F. Shafizadeh, The influence of exchangeable cations on the carbonization of biomass, J. Anal. Appl. Pyrolysis 6 (1984) 217–232, https://doi.org/10.1016/0165-2370(84)80019-4.

[22] L.E. Wise, M. Murphy, A.A. D'Addieco, Chlorite holocellulose, its fractionation and bearing on summative wood analysis and on studies on hemicellulose, Pap. Trade J. 122 (1946) 35–43.

[23] J.A. Pajares, M.A. Díez. Coal and Coke. In: Reedijk, J. (Ed.) Elsevier Reference Module in Chemistry, Molecular Sciences and Chemical Engineering. Waltham, MA: Elsevier, 2014. doi: 10.1016/B978–0-12–409547-2.10968–0.

[24] W.E. Hillis, Heartwood and tree exudates. Springer Series in Wood Science, Springer Verlag, Berlin, 1987 https://link.springer.com/book/10.1007%2F978-3-642-72534-0.

[25] X. Zhang, D. Nguyen, M. Paice, A. Tsang, S. Renaud, Degradation of wood extractives in thermo-mechanical pulp by soybean lipoxygenase, Enzym. Microb. Technol. 40 (4) (2007) 866–873, https://doi.org/10.1016/j.enzmictec.2006.06.021.

[26] B. Klasnja, S. Kopitovic, S. Orlovic, Wood and bark of some poplar and willow clones as fuelwood, Biomass. Bioenergy 23 (2002) 427–432, https://doi.org/10.1016/S0961-9534(02)00069-7.

[27] S. Feng, S. Cheng, Z. Yuan, M. Leitch, C.C. Xu, Valorization of bark for chemicals and materials: a review, Renew. Sustain. Energy Rev. 26 (2013) 560–578, https://doi.org/10.1016/j.rser.2013.06.024.

[28] B.D. González-González, N. Oliveira, I. González, I. Cañellas, H. Sixto, Poplar biomass production in short rotation under irrigation: a case study in the Mediterranean, Biomass Bioenergy 107 (2017) 198–206, https://doi.org/10.1016/j.biombioe.2017.10.004.

[29] M.A. Diez, R. Alvarez, M. Fernández, Biomass derived products as modifiers of the rheological properties of coking coals, Fuel 96 (2012) 306–313, https://doi.org/10.1016/j.fuel.2011.12.065.

[30] J.G. Pohlmann, E. Osório, A.C.F. Vilela, M.A. Diez, A.G. Borrego, Integrating physicochemical information to follow the transformations of biomass upon torrefaction and low-temperature carbonization, Fuel 131 (2014) 17–27, https://doi.org/10.1016/j.fuel.2014.04.067.

[31] M.L. Nelson, R.T. O'Connor, Relation of certain infrared bands to cellulose crystallinity and crystal lattice type. Part I. Spectra of types I, II, III and of amorphous cellulose, J. Appl. Polym. Sci. 8 (1964) 1311–1324.

[32] J. Rodrigues, O. Faix, H. Pereira, Determination of lignin content of Eucalyptus globules wood using FTIR spectroscopy, Holzforsch 52 (1998) 46–50.

[33] J. Xu, M. Huang, Z. Hu, W. Zhang, Y. Li, Y. Yang, Y. Zhou, S. Zhou, Z. Ma, Prediction and modeling of the basic properties of biomass after torrefaction pretreatment, J. Anal. Appl. Pyrolysis 159 (2021), 105287, https://doi.org/10.1016/j.jaap.2021.105287.

[34] T. Sebio-Puñal, S. Naya, J. López-Beceiro, J. Tarrió-Saavedra, R. Artiaga, Thermogravimetric analysis of wood, holocellulose, and lignin from five wood

species, J. Therm. Anal. Calorim. 109 (2012) 1163–1167, https://doi.org/10.1007/s10973-011-2133-1.

[35] K. Raveendran, A. Ganesh, K.C. Khilar, Pyrolysis characteristics of biomass and biomass components, Fuel 75 (8) (1996) 987–998, https://doi.org/10.1016/0016-2361(96)00030-0.

[36] N. Shimada, H. Kawamoto, S. Saka, Different action of alkaline/alkaline earth metal chlorides on cellulose pyrolysis, J. Anal. Appl. Pyrolysis 81 (2008) 80–87, https://doi.org/10.1016/j.jaap.2007.09.005.

[37] H. Chen, Z. Liu, X. Chen, Y. Chen, Z. Dong, X. Wang, H. Yang, Comparative pyrolysis behaviors of stalk, wood and shell biomass: correlation of cellulose crystallinity and reaction kinetics, Bioresour. Technol. 310 (2020), 123498, https://doi.org/10.1016/j.biortech.2020.123498.

[38] P. Giudicianni, V. Gargiulo, C.M. Grottola, M. Alfè, A.I. Ferreiro, M. Abreu Almeida Mendes, M. Fagnano, R. Ragucci, Inherent metal elements in biomass pyrolysis: a review, Energy Fuels (2021) 5407–5478, https://doi.org/10.1021/acs.energyfuels.0c04046.

[39] E. Leng, Y. Zhang, Y. Peng, X. Gong, M. Mao, X. Li, Y. Yu, In situ structural changes of crystalline and amorphous cellulose during slow pyrolysis at low temperatures, Fuel 216 (2018) 313–321, https://doi.org/10.1016/j.fuel.2017.11.083.

[40] T. Faravelli, A. Frassoldati, G. Migliavacca, E. Ranzi, Detailed kinetic modeling of the thermal degradation of lignins, Biomass-.-. Bioenergy 34 (2010) 290–301, https://doi.org/10.1016/j.biombioe.2009.10.018.

[41] S. Chu, A.V. Subrahmanyam, G.W. Huber, The pyrolysis chemistry of a β-O-4 type oligomeric lignin model compound, Green. Chem. 15 (2013) 125, https://doi.org/10.1039/C2GC36332A.

[42] J.Y. Kim, S. Oh, H. Hwang, U.J. Kim, J.W. Choi, Structural features and thermal degradation properties of various lignin macromolecules obtained from poplar wood (*Populus albaglandulosa*), Polym. Degrad. Stab. 98 (2013) 1671–1678, https://doi.org/10.1016/j.polymdegradstab.2013.06.008.

[43] M. Balat, Mechanisms of thermochemical biomass conversion processes. Part 1: reactions of pyrolysis, Energy Sources, Part A: Recovery, Util., Environ. Eff. 30 (7) (2008) 620–635, https://doi.org/10.1080/15567030600817258.

[44] E. Biagini, F. Barontini, L. Tognotti, Devolatilization of biomass fuels and biomass components studied by TG/FTIR technique, Ind. Eng. Chem. Res. 45 (2006) 4486–4493, https://doi.org/10.1021/ie0514049.

[45] H. Yang, R. Yan, H. Chen, D.H. Lee, C. Zheng, Characteristics of hemicellulose, cellulose and lignin pyrolysis, Fuel 86 (2007) 1781–1788, https://doi.org/10.1016/j.fuel.2006.12.013.

[46] J.L. Wen, S.L. Sun, T.Q. Yuan, R.C. Sun, Structural elucidation of whole lignin from Eucalyptus based on preswelling and enzymatic hydrolysis, Green Chem. 17 (2015) 1589–1596. https://doi.org/10.1039/c4gc01889c.

[47] H. Yokoi, Y. Ishida, H. Ohtani, S. Tsuge, T. Sonoda, T. Ona, Characterization of within-tree variation of lignin components in *Eucalyptus camaldulensis* by pyrolysis–gas chromatography, Analyst 124 (1999) 669–674, https://doi.org/10.1039/A809217F.

[48] W.L. Wang, X.Y. Ren, Y.Z. Che, J.M. Chang, J.S. Gou, Kinetics and FTIR characteristics of the pyrolysis process of poplar wood, For. Sci. Pract. 15 (1) (2013) 70–75, https://doi.org/10.1007/s11632-013-0112-2.

[49] P.E.A. Debiagi, C. Pecchi, G. Gentile, A. Frassoldati, A. Cuoci, T. Faravelli, E. Ranzi, Extractives extend the applicability of multistep kinetic scheme of biomass pyrolysis, Energy Fuels 29 (2015) 6544–6555, https://doi.org/10.1021/acs.energyfuels.5b01753.

[50] B. Cagnon, X. Py, A. Guillot, F. Stoeckli, G. Chambat, Contributions of hemicellulose, cellulose and lignin to the mass and the porous properties of chars and steam activated carbons from various lignocellulosic precursors, Bioresour. Technol. 100 (2009) 292–298, https://doi.org/10.1016/j.biortech.2008.06.009.